
Article:
Chen, C., Zhang, J., Chu, X. orcid.org/0000-0003-1863-6149 et al. (1 more author) (2021) On the optimal base-station height in mmWave small-cell networks considering cylindrical blockage effects. IEEE Transactions on Vehicular Technology, 70 (9). pp. 9588-9592. ISSN 0018-9545

https://doi.org/10.1109/TVT.2021.3098626

On the Optimal Base-station Height in mmWave Small-cell Networks Considering Cylindrical Blockage Effects

Chen Chen, *Graduate Student Member, IEEE*, Jiliang Zhang, *Senior Member, IEEE,* Xiaoli Chu, *Senior Member, IEEE,* and Jie Zhang, *Senior Member, IEEE*

***Abstract*—Small-cell networks (SCNs), especially those operating in millimeter-wave bands, are sensitive to blockages. In this letter, we develop a three-dimensional (3D) SCN model considering blockages to investigate the impact of base-station (BS) height, BS density and blockage density on the downlink coverage probability. More specifically, we model the blockages as cylinders whose locations follow a Poisson point process and model the locations of BSs as a Poisson hole process. We assume that all the BSs are of the same height and the blockage height follows an exponential distribution. Based on the 3D SCN model, we derive the exact integral expression of coverage probability for general SCNs and the closed-form expression of coverage probability for ultra-dense SCNs. Our analytical results are verified to be reliable through simulations. The numerical results quantify the impact of the blockage density and the BS height on the coverage probability. For a small blockage density, elevated BSs always degrade the coverage probability, while the coverage probability first increases and then decreases with the BS height when the blockage density becomes sufficiently large.**

***Index Terms*—Small-cell networks, BS height, blockages, coverage probability, Poisson hole process.**

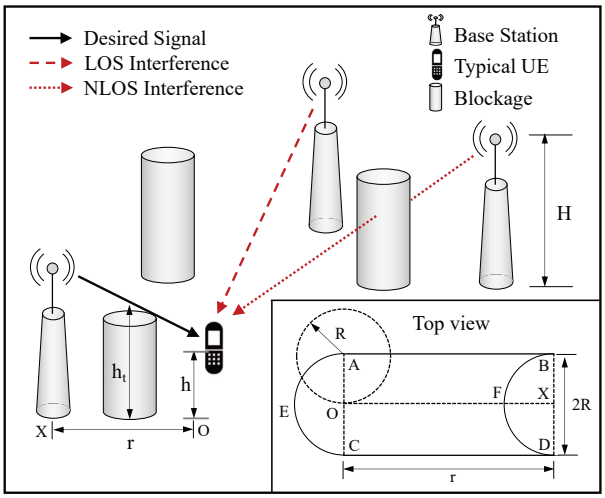

Fig. 1. An illustration of the 3D mmWave small-cell network with blockages.

I. Introduction

Small-cell network (SCN) is considered as one of the most promising technologies to address the 1000× network capacity increase of the fifth generation (5G) mobile networks [1]. The previous work has mainly modeled the cellular networks on a two-dimensional (2D) plane [2]–[4]. Such 2D models work for sparse networks since the link ranges are much larger than the base-station (BS) height. However, in dense SCNs, BSs and user equipments (UEs) communicate in proximity and the link ranges are comparable to the BS heights. Hence, it is of great importance to model the three-dimensional (3D) SCNs and study the impact of the BS height.

A dramatical characteristic of SCN is its irregular distribution, which is commonly modelled with stochastic geometry [5]. A general mathematical framework using homogeneous Poisson point process (PPP) was given in [6], where the SCN was shown to be interference-limited and the increase of the BS density will not affect the coverage probability. In [7], the authors extended the one-tier cellular network to a heterogeneous K-tier network. It was observed that the downlink coverage probability can either increase or decrease with the network densification, depending on different parameter configuration among different tiers.

5G SCNs are expected to operate in millimeter-wave (mmWave) frequencies, i.e., 30–300 GHz, with high penetration loss [8]. Hence, it is crucial to include blockages in the analysis of SCNs. In [9], a distance-dependent line-of-site (LOS) probability function was used to analyze the network coverage probability. It was shown that non-line-of-site links can be beneficial to the coverage probability by blocking the inter-cell interference. A more realistic model of blockages was presented in [10], where the mean value of the signal-to-interference-plus-noise (SINR) was derived. Nevertheless, all of these works modeled the SCNs on a 2D plane without considering the heights of BSs.

Recently, the 3D deployment of small-cells have been studied [11]–[15]. In [11], the authors proposed an analytical framework for the 3D mmWave SCN taking account of both vertical and planar directivities, where the heights of blockages, BSs and UEs were modeled as independent exponential distributions. In [12], [13], it was shown that if the BS height exceeds the UE height, both the coverage probability and area spectral efficiency (ASE) will decrease to zero when the BS density goes to infinity. With this observation, the authors suggested that the BS height should be set the same as the UE height. In [14], the average path loss under the effects of human-body blockages was analyzed using stochastic geometry and validated using a ray-launching method. The results demonstrated that there exists an optimal BS height that minimizes the downlink path loss.

To the best of our knowledge, the potentially coupled impact of the blockage density and the BS height on the coverage probability has not been studied yet. In this letter, we present

Chen Chen, Jiliang Zhang and Xiaoli Chu are with Department of Electronic and Electrical Engineering, The University of Sheffield, Sheffield, S1 4ET, United Kingdom. Jie Zhang is with the Department of Electronic and Electrical Engineering, the University of Sheffield, Sheffield, S1 4ET, UK, and also with Ranplan Wireless Network Design Ltd., Cambridge, CB23 3UY, UK.

This project has received funding from the European Union Horizon 2020 research and innovation program under the ~~Marie Sklodowska Curie~~ grant agreement No. 766231~~ WAVECOMBE H2020 MSCA ITN 2017~~.

a 3D model of downlink mmWave SCN using tools from stochastic geometry, where the locations of blockages and BSs are modelled as a PPP and a Poisson hole process, respectively. Based on the 3D system model, we derive the 3D LOS probability and the probability density function (PDF) of the distance between the typical UE and the serving BS providing the strongest received signal. Subsequently, we derive the tractable expression of the coverage probability, which is then used to analyze the effects of BS density, blockage density and BS height on the coverage probability.

II. System Model

The considered 3D mmWave SCN with blockages is illustrated in Fig. 1. The heights of BSs and UEs are denoted by H and h, respectively, where it is assumed that all the BSs are of the same height and all the UEs are of the same height. For analytical tractability, the blockages are modeled as cylinders, which can be used to model human bodies. We denote the radius of the blockages by R, and the blockage height by H_b. For analytical tractability, we assume that H_b follows an exponential distribution with the parameter μ [11]. The locations of the blockages are distributed following a homogeneous PPP Φ_b on a 2D plane with the density λ_b. The 2D blockage region can be denoted by $S_b = \bigcup_{x\in\Phi_b} B(x,R)$, where $B(x,R)$ is a 2D circle centered at x with the radius R. We assume that the locations of BSs follow a 2D homogeneous Poisson hole process $\Phi_{\rm B}$, i.e., a PPP outside the blockage region. The density of $\Phi_{\rm B}$, i.e., $\lambda_{\rm B}$, can be retained as $\lambda_{bs}\exp(-\lambda_b\pi R^2)$, where λ_{bs} is the spatial density of BSs following a PPP Φ_{bs} when there is no blockage, and $\Phi_{\rm B} = \Phi_{bs}\backslash S_b$ [18]. In this letter, we assume the full buffer traffic model. The more practical scenarios where the packets arrive at the UEs following a stochastic process [16], [17] will be investigated in our future work.

We consider the UE-cell association strategy that connects a UE to the BS providing the strongest downlink received signal. For analytical simplicity, we assume that the blockages are impenetrable. This assumption is reasonable for mmWave communications. Hence, the typical UE will be associated to the closet LOS BS.

The channel model consists of two parts: the large scale path loss and the small scale fading. Without loss of generality, we assume that a typical UE locates at the origin O and the distance between the typical UE and its serving BS is d. The path loss in our 3D system model is expressed as

$$l(d) = \left[d^2 + (H-h)^2\right]^{-\alpha/2}, \tag{1}$$

where α is the path loss exponent. The small scale fading g is modeled by Nakagami-m fading, where m is the shape parameter. The power of g follows the Gamma distribution $\Gamma(m, \frac{1}{m})$, where m is assumed to be an integer [9].

We assume that BSs are equipped with antenna arrays and each UE has a single receiving antenna. The widely used sectored antenna model [9] is adopted to approximate the beamforming pattern, which is denoted by

$$G(\theta) = \begin{cases} G_{\rm M}, & P_{\rm M} = \frac{\theta}{2\pi}, \\ G_{\rm m}, & P_{\rm m} = 1 - P_{\rm M}, \end{cases} \tag{2}$$

where θ is the main lobe beamwidth, $G_{\rm M}$ denotes the main lobe gain, $P_{\rm M}$ is the probability of main lobe, $G_{\rm m}$ denotes the side lobe gain, and $P_{\rm m}$ is the probability of side lobe.

III. Analysis of LOS Probability

In this section, we analyze the LOS probability between the typical UE at the origin O and a BS at distance r under the 3D SCN model.

A. The Horizontal LOS Probability

As shown in Fig. 1, OX is a link from the origin of the 2D plane to a BS location X with distance r, and the horizontal LOS probability is defined as the probability that no blockage intersects OX on the 2D plane.

Lemma 1: The horizontal LOS probability of the link OX is $e^{-\beta r}$.

Proof: Since the BSs distribute following the Poisson hole process, there will be no blockage located in the semicircular region BFD. Hence, a blockage will lie across OX when it is located in the region $ABFDCE$. Denote M as the total number of blockages lying across OX, then M is a Poisson random variable and its mean can be computed as

$$\mathbb{E}(M) = \lambda_b S_{ABFDCE} = 2\lambda_b R r = \beta r, \tag{3}$$

where S_{ABFDCE} is the area of the region $ABFDCE$. The horizontal LOS probability is the probability that $M = 0$, which can be obtained using the properties of Poisson distribution. The LOS probability for general blockages with shapes other than cylinders will be investigated in our future work. ■

B. The 3D LOS Probability

Lemma 2: The 3D LOS probability of the link from the typical UE to the BS at X is given by $e^{-\delta\beta r}$, where $\delta = \frac{e^{-\mu h} - e^{-\mu H}}{\mu(H-h)}$.

Proof: As shown in Fig. 1, if a blockage intersects OX at distance t from O on the 2D plane, it will effectively block the propagation link from the BS to the typical UE when $H_b > h_t$. The conditional probability that a blockage blocks the downlink to the typical UE under the condition that it intersects OX is given by

$$\begin{aligned} \delta &= \frac{1}{r}\int_0^r \mathbb{P}\left[H_b > h_t\right] \mathrm{d}t \\ &\overset{(a)}{=} \frac{1}{r}\int_0^r \left(1 - \int_0^{\frac{hr+(H-h)t}{r}} f_H(H_b)\mathrm{d}H_b\right)\mathrm{d}t \\ &= 1 - \frac{1}{r}\int_0^r \int_0^{\frac{hr+(H-h)t}{r}} \mu e^{-\mu H_b}\mathrm{d}H_b\mathrm{d}t \\ &= \frac{e^{-\mu h} - e^{-\mu H}}{\mu(H-h)}, \end{aligned} \tag{4}$$

where $f_H(H_b)$ is the PDF of H_b. Denote the number of blockages that effectively block the propagation link by $\bar{M}$, then $\bar{M}$ can be considered as an independent thinning of M with the parameter δ [19]. Therefore, $\bar{M}$ is also a Poisson random variable and $\mathbb{E}(\bar{M}) = \delta\beta r$. The 3D LOS probability can be obtained by computing the probability that $\bar{M} = 0$. Note that the derivation of 3D LOS probability under the exponential distribution of blockage height in (4) can be extended to other distributions using (a). ■

IV. Coverage Probability Analysis

In this section, we analyze the downlink coverage probability for SCNs. Firstly, we derive the expression of the PDF of the horizontal distance from the typical UE to the closet LOS BS. Based on the PDF, we obtain the expression of the downlink coverage probability. Moreover, for ultra-dense SCNs, we obtain the closed-form expression of the downlink coverage probability.

A. Coverage Probability of Small-cell Networks

Recall that the distance between the typical UE and the serving BS is denoted by d.

Lemma 3: The PDF of d is computed by $f_d(x) = 2\pi\lambda_{\mathrm{B}} x e^{-[\delta\beta x + 2\pi\lambda_{\mathrm{B}} Q(x)]}$, where $Q(x) = \frac{1}{(\delta\beta)^2}\left[1 - (\delta\beta x + 1)e^{-\delta\beta x}\right]$.

Proof: The complementary cumulative distribution function (CCDF) of d is

$$\begin{aligned}\mathbb{P}(d > x) &= \mathbb{P}[\text{No LOS BS in } B(O,x)] \\ &= \exp\left\{-2\pi\lambda_{\mathrm{B}}\int_0^x e^{-\delta\beta r} r \mathrm{d}r\right\} \\ &= e^{-2\pi\lambda_{\mathrm{B}} Q(x)},\end{aligned} \tag{5}$$

where $B(O,x)$ is the circle centered at O with the radius x. Then we can compute the PDF of d as

$$f_d(x) = \frac{\mathrm{d}(1 - \mathbb{P}(d > x))}{\mathrm{d}(x)} = 2\pi\lambda_{\mathrm{B}} x e^{-[\delta\beta x + 2\pi\lambda_{\mathrm{B}} Q(x)]}, \tag{6}$$

■

We assume that the SCN is interference-limited [6]. Hence, the coverage probability is the probability that the SIR of the typical UE is higher than a threshold T, which can be expressed as

$$\mathrm{P}_{\mathrm{COV}} = \mathbb{P}(\mathrm{SIR} > T). \tag{7}$$

We further assume that the maximum array gain G_{M} can always be obtained from the serving BS to the typical UE [9]. Given that $d = x$, the SIR is defined as

$$\mathrm{SIR} = \frac{g_0 G_{\mathrm{M}}\left[x^2 + (H-h)^2\right]^{-\alpha/2}}{\sum_{i\in\Phi_{\mathrm{L}}\setminus \mathrm{B}_0} g_i G(\theta)\left[R_i^2 + (H-h)^2\right]^{-\alpha/2}}, \tag{8}$$

where g_0 and g_i are the fading power gains from the typical UE to the serving BS B_0 and to the interfering BS B_i, respectively, R_i is the distance from the interfering BS B_i to the typical UE, and Φ_{L} is the set of LOS BSs.

Theorem 1: The downlink coverage probability of a SCN is given by

$$\begin{aligned}\mathrm{P}_{\mathrm{COV}}(H,\lambda_{\mathrm{B}},\lambda_{\mathrm{b}}) \approx &\sum_{n=1}^{m}(-1)^{n+1}\binom{m}{n} \\ &\times \int_0^\infty \exp\left\{-2\pi\lambda_{\mathrm{B}}\int_x^\infty F(T,x,t)e^{-\delta\beta t} t\mathrm{d}t\right\} f_d(x)\mathrm{d}x,\end{aligned} \tag{9}$$

where

$$F(T,x,t) = 1 - \left[1 + \frac{\zeta n T G_{\mathrm{I}}}{m}\left(\frac{x^2 + (H-h)^2}{t^2 + (H-h)^2}\right)^{\frac{\alpha}{2}}\right]^{-m}, \tag{10}$$

$\zeta = m(m!)^{-\frac{1}{m}}$ and $G_{\mathrm{I}} = \frac{G_{\mathrm{M}}P_{\mathrm{M}} + G_{\mathrm{m}}P_{\mathrm{m}}}{G_{\mathrm{M}}}$.

Proof: See Appendix A. ■

B. Coverage Probability of Ultra-dense Small-cell Networks

When the network becomes ultra-dense, we assume that the BS density is much higher than the blockage density, such that the effects of blockages is negligible.

Theorem 2: The closed-form coverage probability of the ultra-dense small-cell networks is given by

$$\begin{aligned}\mathrm{P}_{\mathrm{COV\_U}}(H,\lambda_{\mathrm{B}}) \approx &\sum_{n=1}^{m}(-1)^{n+1}\binom{m}{n} \\ &\times \frac{\exp\left\{\pi\lambda_{\mathrm{B}}(H-h)^2\left(1 - \frac{2s(\zeta n T G_{\mathrm{I}})^{\frac{2}{\alpha}}}{\alpha}\right)\right\}}{2s(\zeta n T G_{\mathrm{I}})^{\frac{2}{\alpha}}/\alpha},\end{aligned} \tag{11}$$

where $s = \Gamma\left(-\frac{2}{\alpha}, \zeta n T G_{\mathrm{I}}\right) - \Gamma\left(-\frac{2}{\alpha}\right)$, $\Gamma(z,x) = \int_x^\infty t^{z-1}e^{-t}\mathrm{d}t$ is the incomplete gamma function and $\Gamma(z) = \int_0^\infty t^{z-1}e^{-t}\mathrm{d}t$ is the standard gamma function.

Proof: See Appendix B. ■

V. Numerical Results

In this section, we validate our analytical expressions with Monte Carlo simulations. We set the the UE height as $h = 1$ m, the parameter of the blockage height distribution as $\mu = 1/1.5$, the coverage probability threshold as $T = 5$ dB, path loss exponent $\alpha = 2$ and the parameter of the Nakagami-m fading as $m = 3$. The default values of the radius of blockages, BS density with no blockage, and blockage density are set as $R = 2$ m, $\lambda_{\mathrm{bs}} = 10^{-2}$ BS/m^2, and $\lambda_{\mathrm{b}} = 2\times10^{-2}$ blockage/m^2, respectively. The default parameters of beamforming are set as $G_{\mathrm{M}} = 10$ dB, $G_{\mathrm{m}} = -10$ dB, and $\theta = 30°$. In Fig. 2, the coverage probability for our proposed 3D SCN is evaluated. We can see that the simulation results match well with our analytical curves.

In Fig. 3, we show the influence of the blockage density to the coverage probability for $H = 1$ m, $H = 2$ m, $H = 3$ m and $H = 4$ m, respectively. With the increase of the blockage density, the coverage probability first increases and then decreases. This indicates that a low blockage density is beneficial for the network coverage probability, however, when the blockage density becomes sufficiently high, it will degrade the coverage probability. We can also find that for a given BS

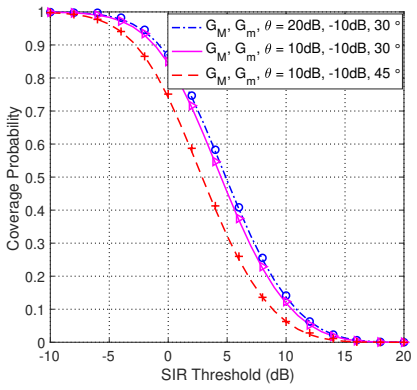

Fig. 2. The coverage probability vs. the SIR threshold for $\lambda_b = 10^{-2}$ blockage/m^2.

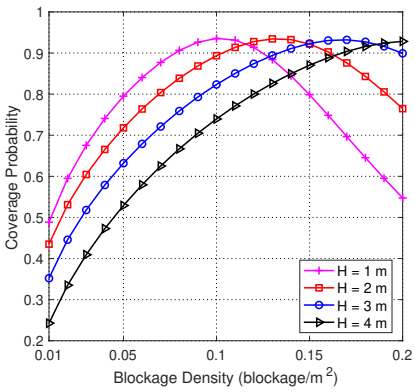

Fig. 3. The coverage probability vs. the blockage density for $R = 1$ m.

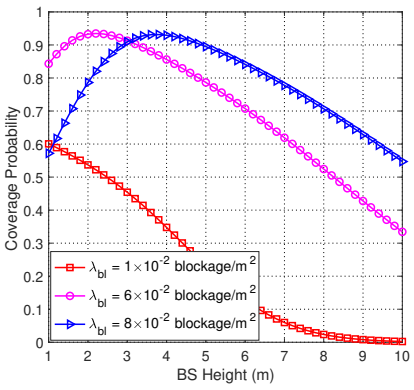

Fig. 4. The coverage probability vs. the BS height for $R = 2$ m.

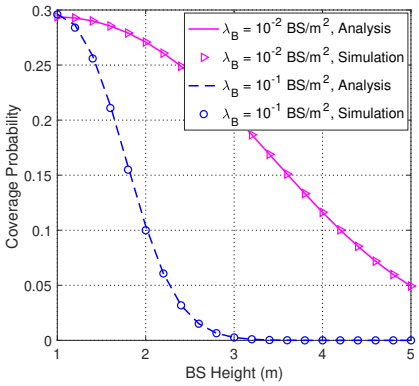

Fig. 5. The coverage probability vs. the BS height in ultra-dense SCNs.

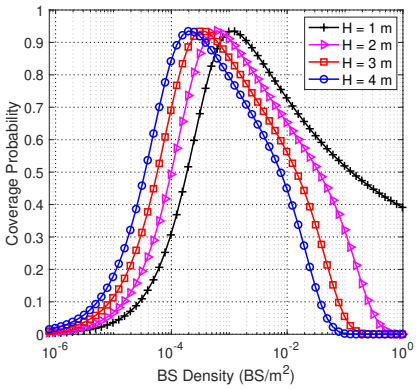

Fig. 6. The coverage probability vs. the BS density.

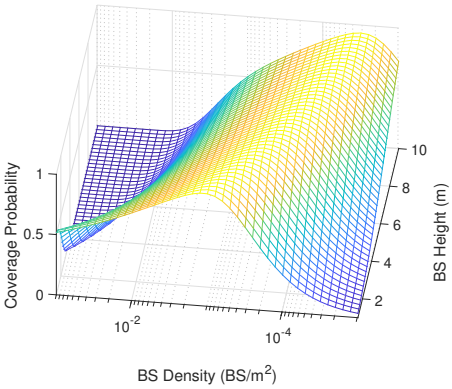

Fig. 7. The coverage probability vs. the BS height and BS density.

density, the optimal blockage density will be higher when the BS height increases.

In Fig. 4, we show the influence of the BS height to the coverage probability. It is obtained that for a small blockage density, the coverage probability will monotonically decrease with the BS height. While for the higher blockage densities, the coverage probability will first increase and then decreases with the BS height. This demonstrates that for a given BS density, when the blockage density is beneficial for the coverage probability, the BS height should be identical with the UE height to avoid the coverage probability loss. However, when the blockage density becomes harmful, there exists an optimal BS height higher than the UE height that maximizes the coverage probability. The optimal BS heights can be found by computing $\frac{\mathrm{dP_{COV}}(H,\lambda_\mathrm{B},\lambda_\mathrm{b})}{\mathrm{d}H} = 0$ and numerically obtained using the bisection search [21]. The numerical results are 2.2 m and 3.73 m for $\lambda_b = 6 \times 10^{-2}$ blockage/m^2 and $\lambda_b = 8 \times 10^{-2}$ blockage/m^2, respectively. Fig. 5 shows the numerical results for the ultra-dense small-cell networks where the blockages are negligible. It is observed that the coverage probability monotonically decreases with the BS height, which matches the conclusion obtained from Fig. 4.

From Fig. 6, we observe that for a given blockage density, the coverage probability first increases and then decreases with the BS density. This can be intuitively explained that a higher BS density brings higher LOS probability, however, increasing BS density also leads to more interference from LOS BSs. The coverage probability will decline when the loss resulting from the interference exceeds the gain of the LOS received signals. The optimal BS densities can be found by computing $\frac{\mathrm{dP_{COV}}(H,\lambda_\mathrm{B},\lambda_\mathrm{b})}{\mathrm{d}\lambda_\mathrm{B}} = 0$. The numerical results are 1.1×10^{-3} BS/m^2, 6×10^{-4} BS/m^2, 3.4×10^{-4} BS/m^2 and 2×10^{-4} BS/m^2 for $H = 1$ m, $H = 2$ m, $H = 3$ m and $H = 4$ m, respectively. Moreover, we can observe that a higher BS height leads to a lower optimal BS density. Hence, for a given blockage density, less BSs are needed to be deployed to obtain a maximum coverage probability when increasing the BS height.

In Fig. 7, we plot the 3D figure to show the joint impact of the BS density and BS height. It can be observed that for a given BS height range, there exists a corresponding BS density range that can lead to the maximum coverage probability. This can provide guidance for the joint optimization of BS density and BS height.

VI. Conclusion and Future Works

In this letter, we have presented a 3D model of mmWave SCNs under the impact of random blockages. We derived the downlink coverage probability in an integral form for general SCNs and in closed-form for ultra-dense SCNs. Our analytical and simulation results showed that for a small blockage density, the increasing BS height always degrades the coverage probability. However, when the blockage density becomes

sufficiently large, the coverage probability first increases and then decreases with the BS height. We have also observed that for a given range of BS heights, there exists an optimal range of BS densities that maximize the coverage probability.

In our future work, we will include the modeling of more general blockages. Additionally, we will extend this work to 3D heterogeneous mmWave SCNs.

APPENDIX

A. Proof of Theorem 1

Plugging (8) into (7), we have

$$\begin{aligned}&\mathrm{P}_{\mathrm{COV}}(H,\lambda_{\mathrm{B}},\lambda_{\mathrm{b}})\\&=\int_0^{\infty}\mathbb{P}\left[\frac{g_0 G_{\mathrm{M}} l(x)}{\sum_{i\in\Phi_{\mathrm{L}}\setminus\mathrm{B}_0} g_i G(\theta) l(R_i)}>T\right] f_d(x)\mathrm{d}x\\&=\int_0^{\infty}\mathbb{P}\left[g_0>TG_{\mathrm{I}} l(x)^{-1}\sum_{i\in\Phi_{\mathrm{L}}\setminus\mathrm{B}_0} g_i l(R_i)\right] f_d(x)\mathrm{d}x, \quad (12)\end{aligned}$$

where

$$\begin{aligned}&\mathbb{P}\left[g_0>TG_{\mathrm{I}} l(x)^{-1}\sum_{i\in\Phi_{\mathrm{L}}\setminus\mathrm{B}_0} g_i l(R_i)\right]\\&\overset{(a)}{<}1-\mathbb{E}\left[\left(1-e^{-\zeta TG_{\mathrm{I}} l(x)^{-1}\sum_{i\in\Phi_{\mathrm{L}}\setminus\mathrm{B}_0} g_i l(R_i)}\right)^m\right]\\&\overset{(b)}{=}\sum_{n=1}^{m}(-1)^{n+1}\tbinom{m}{n}\mathbb{E}\left[e^{-\zeta nTG_{\mathrm{I}} l(x)^{-1}\sum_{i\in\Phi_{\mathrm{L}}\setminus\mathrm{B}_0} g_i l(R_i)}\right].\end{aligned} \quad (13)$$

Therein, (a) comes from that for a gamma random variable g with parameter m, $\mathbb{P}(g<x)$ can be lower-bounded by $\mathbb{P}(g<x)>(1-e^{-ax})^m$, where $x>0$ and $a=m(m!)^{-\frac{1}{m}}$ [20]. (b) follows from Binomial series expansion.

Applying the probability generating functional of homogeneous PPP, we have

$$\begin{aligned}&\mathbb{E}\left[e^{-\zeta nTG_{\mathrm{I}} l(x)^{-1}\sum_{i\in\Phi_{\mathrm{L}}\setminus\mathrm{B}_0} g_i l(R_i)}\right]\\&=\exp\left\{-2\pi\lambda_{\mathrm{B}}\int_x^{\infty}\left(1-\mathbb{E}_g\left[e^{-\zeta nTG_{\mathrm{I}} g l(t)/l(x)}\right]\right)e^{-\delta\beta t}t\mathrm{d}t\right\}\\&\overset{(a)}{=}\exp\left\{-2\pi\lambda_{\mathrm{B}}\int_x^{\infty}\left[1-\left[1+\frac{\zeta nTG_{\mathrm{I}}\frac{l(t)}{l(x)}}{m}\right]^{-m}\right]e^{-\delta\beta t}t\mathrm{d}t\right\},\end{aligned} \quad (14)$$

where (a) come from the moment generating function of the gamma random variable g.

B. Proof of Theorem 2

According to the assumption of ultra-dense SCNs, all the BSs will be LOS BSs. The coverage probability is computed as

$$\begin{aligned}&\mathrm{P}_{\mathrm{COV\_U}}(H,\lambda_{\mathrm{B}})=\\&\int_0^{\infty}\mathbb{P}\left[\frac{g_0 G_{\mathrm{M}} l(x)}{\sum_{i\in\Phi_{\mathrm{B}}\setminus\mathrm{B}_0} g_i G(\theta) l(R_i)}>T\right] 2\pi\lambda_{\mathrm{B}} x e^{-\pi\lambda_{\mathrm{B}}x^2}\mathrm{d}x.\end{aligned} \quad (15)$$

Following (12), we have

$$\begin{aligned}&\mathbb{P}\left[\frac{g_0 G_{\mathrm{M}} l(x)}{\sum_{i\in\Phi_{\mathrm{B}}\setminus\mathrm{B}_0} g_i G(\theta) l(R_i)}>T\right]\\&=\sum_{n=1}^{m}(-1)^{n+1}\tbinom{m}{n}\mathbb{E}\left[e^{-\zeta nTG_{\mathrm{I}} l(x)^{-1}\sum_{i\in\Phi_{\mathrm{B}}\setminus\mathrm{B}_0} g_i l(R_i)}\right],\end{aligned} \quad (16)$$

where $\mathbb{E}\left[e^{-\zeta nTG_{\mathrm{I}} l(x)^{-1}\sum_{i\in\Phi_{\mathrm{B}}\setminus\mathrm{B}_0} g_i l(R_i)}\right]$ is computed by

$$\begin{aligned}&\mathbb{E}\left[e^{-\zeta nTG_{\mathrm{I}} l(x)^{-1}\sum_{i\in\Phi_{\mathrm{B}}\setminus\mathrm{B}_0} g_i l(R_i)}\right]\\&=\exp\left\{-2\pi\lambda_{\mathrm{B}}\int_x^{\infty}\left(1-\mathbb{E}_g\left[e^{-\zeta nTG_{\mathrm{I}} g l(t)/l(x)}\right]\right)t\mathrm{d}t\right\}\\&\overset{(a)}{>}\exp\left\{-2\pi\lambda_{\mathrm{B}}\int_x^{\infty}\left(1-e^{-\zeta nTG_{\mathrm{I}} l(t)/l(x)}\right)t\mathrm{d}t\right\}\\&\overset{(b)}{=}\exp\left\{-\pi\lambda_{\mathrm{B}}\int_{x^2}^{\infty}\left(1-e^{-A(t+h_d^2)}\right)\mathrm{d}t\right\}\\&\overset{(c)}{=}\exp\left\{\pi\lambda_{\mathrm{B}}A^{\frac{2}{\alpha}}\int_0^{A(x^2+h_d^2)^{-\frac{\alpha}{2}}}\int_0^{r}e^{-u}r^{-\frac{2}{\alpha}-1}\mathrm{d}u\mathrm{d}r\right\}\\&\overset{(d)}{=}\exp\Bigg\{\pi\lambda_{\mathrm{B}}(x^2+h_d^2)\\&-\frac{2\pi\lambda_{\mathrm{B}}A^{\frac{2}{\alpha}}}{\alpha}\left[\Gamma\left(-\frac{2}{\alpha},\zeta nTG_{\mathrm{I}}\right)-\Gamma\left(-\frac{2}{\alpha}\right)\right]\Bigg\}.\end{aligned} \quad (17)$$

Therein, (a) comes from $\left(1+\frac{k}{x}\right)^{-x}>e^{-k}$ for $k>0$, in (b), we define $A=\zeta nTG_{\mathrm{I}}/l(x)$ and $h_d=H-h$, (c) is obtained by using the substitution $A(t+h_d^2)\to r$ and (d) follows from the swapping of integration order in (c). By substituting (16), (17) into (15), the closed-form expression of coverage probability can be obtained.

REFERENCES

[1] J. G. Andrews, X. Zhang, G. D. Durgin and A. K. Gupta, "Are we approaching the fundamental limits of wireless network densification?" *IEEE Commun. Mag.,* vol. 54, no. 10, pp. 184-190, Oct. 2016.

[2] X. Zhang and J. G. Andrews, "Downlink cellular network analysis with multi-slope path loss models," *IEEE Trans. Commun.*, vol. 63, no. 5, pp. 1881-1894, May. 2015.

[3] J. Liu, M. Sheng, L. Liu, and J. Li, "Effect of densification on cellular network performance with bounded pathloss model," *IEEE Commun. Lett.*, vol. 21, no. 2, pp. 346-349, Feb. 2017.

[4] C. Chen, S. Yang, J. Zhang, X. Chu, and J. Zhang, "Tractable performance analysis of small-cell networks with a novel bounded path loss model," *Electron. Lett.*, vol. 56, no. 2, pp. 105-107, 23 01 2020.

[5] M. Kamel, W. Hamouda and A. Youssef, "Ultra-dense networks: a survey," *IEEE Commun. Surveys Tut.,* vol. 18, no. 4, pp. 2522-2545, Fourthquarter 2016.

[6] J. G. Andrews, F. Baccelli, and R. K. Ganti, "A tractable approach to coverage and rate in cellular networks," *IEEE Trans. Commun.,* vol. 59, no. 11, pp. 3122-3134, Nov. 2011.

[7] H. S. Dhillon, R. K. Ganti, F. Baccelli, and J. G. Andrews, "Modeling and analysis of K-tier downlink heterogeneous cellular networks," *IEEE J. Sel. Areas Commun.,* vol. 30, no. 3, pp. 550-560, Apr. 2012.

[8] J. G. Andrews *et al*., "What will 5G be?" *IEEE J. Sel. Areas Commun.*, vol. 32, no. 6, pp. 1065-1082, Jun. 2014.

[9] T. Bai and R. W. Heath, Jr., "Coverage and rate analysis for millimeter-wave cellular networks," *IEEE Trans. Wireless Commun.*, vol. 14, no. 2, pp. 1100-1114, Feb. 2015.

[10] V. Petrov, M. Komarov, D. Moltchanov, J. M. Jornet and Y. Koucheryavy, "Interference and SINR in millimeter wave and terahertz communication systems with blocking and directional antennas," *IEEE Trans. Wireless Commun.,* vol. 16, no. 3, pp. 1791-1808, Mar. 2017.

[11] R. Kovalchukov *et al.*, "Evaluating SIR in 3D millimeter-wave deployments: direct modeling and feasible approximations," *IEEE Trans. Wireless Commun.,* vol. 18, no. 2, pp. 879-896, Feb. 2019.
[12] M. Ding and D. López-Pérez, "Performance impact of base station antenna heights in dense cellular networks," *IEEE Trans. Wireless Commun.,* vol. 16, no. 12, pp. 8147-8161, Dec. 2017.
[13] J. Liu, M. Sheng, K. Wang, and J. Li, "The impact of antenna height difference on the performance of downlink cellular networks," in *Proc. IEEE Globecom,* Singapore, Dec. 2017, pp. 1-7
[14] M. Gapeyenko *et al.*, "Analysis of human-body blockage in urban millimeter-wave cellular communications," in *Proc. IEEE Int. Conf. Commun. (ICC)*, 2016, pp. 1-7.
[15] J. Lee, X. Zhang, and F. Baccelli, "A 3D spatial model for in-building wireless networks with correlated shadowing," *IEEE Trans. Wireless Commun.,* vol. 15, no. 11, pp. 7778-7793, Nov. 2016.
[16] Y. Zhong, T. Q. S. Quek and X. Ge, "Heterogeneous cellular networks with spatio-temporal traffic: delay analysis and scheduling," *IEEE J. Sel. Areas Commun.*, vol. 35, no. 6, pp. 1373-1386, Jun. 2017.
[17] Y. Zhong, G. Mao, X. Ge and F. Zheng, "Spatio-temporal modeling for massive and sporadic access," Jul. 2020, arXiv:2001.11783. [Online]. Available: https://arxiv.org/abs/2001.11783
[18] Y. Zhong, T. Q. S. Quek and W. Zhang, "Complementary networking for C-RAN: spectrum efficiency, delay and system cost," *IEEE Trans. Wireless Commun.,* vol. 16, no. 7, pp. 4639-4653, Jul. 2017.
[19] T. Bai, R. Vaze, and R. W. Heath, "Analysis of blockage effects on urban cellular networks," *IEEE Trans. Wireless Commun.,* vol. 13, no. 9, pp. 5070-5083, Sep. 2014.
[20] A. Thornburg, T. Bai, and R. Heath, "Performance analysis of outdoor mmWave ad hoc networks," *IEEE Trans. Signal Process.*, vol. 64, no. 15, pp. 4065-4079, Aug. 2016.
[21] R. L. Burden and J. D. Faires, "Numerical analysis (3rd Ed.)," *PWS Publishers*, 1985.